Ionics (2022) 28:4579–4585
https://doi.org/10.1007/s11581-022-04715-z

ORIGINAL PAPER

Improved electrochemical performance of $LiFePO_4$/carbon cathode for lithium-ion batteries

Xuyan Liu[1] · Ruipeng Zhao[1] · Yijie Xia[1] · Qiang Li[1]

Received: 5 June 2022 / Accepted: 3 August 2022 / Published online: 17 August 2022

Abstract

$LiFePO_4$/carbon (LFP/C) composites with different carbon contents are obtained through a carbothermic reduction process using glucose as carbon source. The effect of carbon content on the performance of LFP is investigated through structure and electrochemical characterization analysis. It is obvious that LFP/C composites significantly enhance the electrochemical performance compared with the unmodified LFP as the carbon content increases. In particular, LFP/C with 15% carbon content (LFP/C-15) exhibits the highest initial discharge specific capacity and the most superior capacity retention rate, with a discharge capacity of 160.7 mAh g^{-1} and a capacity retention rate of 82.1% after 100 cycles at 0.1 C. Moreover, the discharge capacity is already very close to the theoretical specific capacity of $LiFePO_4$ (170 mAh g^{-1}). However, when the carbon content reaches 20%, the electrochemical performance decreases instead, indicating that excessive carbon content has the opposite effect on the improvement of material performance. Hence, the carbon content plays a crucial role in the future improvement of the material properties.

Keywords $LiFePO_4$ · Carbon coating · Carbon content · Excellent electrochemical performance

Introduction

In the past few decades, olivine-structured $LiFePO_4$ (LFP) has been intensively investigated and it was considered to be one of the most promising cathode materials of Li-ion batteries since it was initially introduced by Goodenough's research group [1]. $LiFePO_4$ have been widely applied in various industries due to high safety, relative high energy density, lower cost, non-toxicity, and excellent thermal stability [2–7]. Nowadays, the growing market of electric vehicles (EV) and hybrid electric vehicles (HEV) has enhanced the demand for $LiFePO_4$, so that it has enormous potential in the electric vehicle industry [8–11]. The two-phase reaction means that during charging, Li ions are extracted from $LiFePO_4$ cathode to the anode (typically, graphite) across the electrolyte, and vice versa upon discharging [1]. Based on a two-phase reaction, $LiFePO_4$ exhibits a high theoretical specific capacity of 170 mAh g^{-1} and a discharge plateau voltage of about 3.4 V [12–15].

In spite of these advantages, it still suffers from some problems such as low electric conductivity (~10^{-9} S cm^{-1}) and slow diffusion of lithium ion across the two-phase boundary, which brings big obstacles to the practical application [16–20]. To further overcome these limitations and improve the performance of LFP, it is of great importance to come up with some ways. Recent researches have reported that the inherent drawbacks can be remedied by carbon coating, foreign hetero-atom doping, and hierarchical nano-/micro-structure assembly. Liu T. [21] et al. investigated the effect of three different carbon materials on the depolarization effect and electrochemical properties of $LiFePO_4$ cathode. The results showed that the graphene nano-sheet (GN)-modified materials exhibited the best performance, with the discharge capacity of LFP/CNs-Al reaching 122 mAh g^{-1} at 5 C; however, the discharge capacity of LFP-Al was only 49.2 mAh g^{-1}. Zhang K. [22] et al. significantly improved the electrochemical performance of $LiFePO_4$ by a conformal coating consisting of N-doped carbon and conventional graphene. The specific capacity at 0.1 C reached 171.9 mAh g^{-1}, which has exceeded the theoretical capacity of the material. And the cycle retention rate reached

✉ Xuyan Liu
lxuyan@163.com

[1] School of Mechanical Engineering, University of Shanghai for Science and Technology, No. 516, Jun Gong Road, Shanghai 200093, China

95.8% after 1000 cycles at 10 C. Ni J. [23] et al. prepared Mg-doped $LiFePO_4$ samples using a specially designed two-step solid-phase reaction. The dopants were located at two different sites, which were named as $Li_{1-2x}Mg_xFePO_4$ and $LiFe_{1-x}Mg_xPO_4$, respectively. The results showed that doping in Fe site affords a better capacity delivery and reversibility than in Li site in the $LiFePO_4$. Meanwhile, the $LiFe_{0.98}Mg_{0.02}PO_4$ exhibits a much higher reversible capacity of 156 mAh g^{-1} than the undoped one (97 mAh g^{-1}). Liu Y. [24] et al. successfully synthesized $LiFe_{1-x}Ni_xPO_4$/C composites by a hydrothermal method and the effect of Ni content was investigated. Compared with pure $LiFePO_4$, the $LiFe_{0.97}Ni_{0.03}PO_4$/C composite has higher capacity and better cycling. The specific capacity was 169.5 mAh g^{-1} at 0.2 C and could reach 122.9 mAh g^{-1} at 5 C. Even at 10 C, the capacity retention was 93.9% after 200 cycles. Khan S. [25] et al. prepared composite electrodes consisting of nano-sized $LiFePO_4$ embedded in ordered mesoporous carbon and non-nitrogen-doped mesoporous carbon (LFP/MNC-31 and LFP/CMK-3). Electrochemical studies reveal that the Li-ion diffusion coefficient values in LFP/MNC-31 composite are remarkably higher compared to LFP/CMK-3 as well as LFP. It shows relatively better electrochemical properties in terms of specific capacity, rate capability, and cyclic stability.

Among various methods, carbon coating has become the most effective and inexpensive modification method, which effectively enhances the conductivity of $LiFePO_4$ by constructing a conduction network. The content of carbon additives has a significant impact on obtaining $LiFePO_4$/carbon (LFP/C) composites with excellent electrochemical properties. The appropriate carbon additive can form a perfect conductive carbon layer covering the surface of $LiFePO_4$. The conductive carbon layer can restrict the size of the particles so that the size of the material is more uniform, and it can form a good conductive network to improve the conductivity. However, excessive carbon additives have the opposite effect on the electrochemical properties of the material.

In this work, LFP/C composites with different carbon contents are successfully prepared through carbothermal reduction using glucose as the carbon source, and the effect of carbon contents on the properties of LFP/C is investigated. As a cathode material for LIBs, the as-prepared LFP/C remarkably improves reversible specific capacity, rate capability and capacity retention rate compared, which is attributed to excellent conductive properties of the conductive network formed by carbon coating. Among them, the discharge capacity of LFP/C with 15% carbon content at 0.1 C is very close to the theoretical specific capacity of $LiFePO_4$ and shows excellent cycle efficiency. Therefore, carbon coating is a very effective and promising way to enhance the performance of $LiFePO_4$. Moreover, the carbon content plays a crucial role in the improvement of the material performance.

Experimental details

Preparation of materials

$LiFePO_4$ was obtained by using $FePO_4$ as precursor and adding a lithium source. Firstly, stoichiometric amount of 5.60 g $FeSO_4{\cdot}7H_2O$ in deionized water (~ 15 mL) with constant stirring was dissolved. Of the 98 wt% H_3PO_4 solution, 0.5 mL was dropped into the beaker. In order to dilute the solution sufficiently, 15 mL deionized water was introduced into the above solution. Then, $FeSO_4{\cdot}7H_2O$ solution was slowly dropped in H_3PO_4 solution with stirring. $FePO_4{\cdot}2H_2O$ was gained after the product was washed, centrifuged, and dried, respectively. Finally, $FePO_4$ can be prepared by heating the $FePO_4{\cdot}2H_2O$ powders at 450 °C. $LiFePO_4$ was prepared through a carbothermic reduction process using Li_2CO_3 and as-prepared $FePO_4$ as raw material with a molar ratio of 1:2. The carbothermic reduction process was described below. $FePO_4$ was added to a mortar and ground for 1 h. Then, 0.89 g Li_2CO_3 and 0.72 g $C_6H_{12}O_6$ were, respectively, introduced into the mortar and ground for 3 h. Subsequently, after heating the above mixture in a tube furnace at 600 °C for 8 h, LFP/C composite materials were able to be synthesized. To remove the carbon layer from the surface of $LiFePO_4$/C, it was fully dissolved in an aqueous solution and ultrasonic treatment for 1 h. After drying at 110 °C for 12 h, the black LFP powder could be produced.

To investigate the effect of carbon contents on the properties of $LiFePO_4$/C composites, glucose was added as carbon source at different ratios of 0%, 5%, 10%, 15%, and 20%. First, 1 g $LiFePO_4$ was added in a mortar and ground for 1 h. Then 0 g, 0.05 g, 0.1 g, 0.15 g, and 0.2 g glucose were, respectively, added in the above mortar and ground for 2 h. After drying for 2 h, it was putted in a tube furnace and heated to 700 °C at 5 °C/min. $LiFePO_4$/C powder was obtained after heating for 8 h and cooling to room temperature. The above-prepared materials were named as LFP (0 g), LFP/C-5 (0.05 g), LFP/C-10 (0.1 g), LFP/C-15 (0.15 g), and LFP/C-20 (0.2 g).

Structural characterization

The structural characterization of all active materials was identified by a scanning electron microscope (SEM; JEOL JSM-7000F, Japan) and X-ray diffraction (XRD) using a Rigaku D/Max-2500 X-ray diffractometer with Cu Kα radiation ($\lambda = 1.5$ Å).

Electrochemical characterization

The electrode materials were prepared by mixing 10 wt% acetylene black (Tianjin Tianyi Century Chemical

Products Technology Development Co., Ltd.), 80 wt% active materials, and 10 wt% poly (vinylidenedifluoride) (Aldrich Chemical Co., Ltd.) in ethanol. The as-prepared slurries were uniformly coated onto the copper foil and dried at 80 °C in vacuum for 24 h. Generally, the lithium metal foil played the role of a counter electrode, the Celgard 2300 film functioned as a separator, and 1 M $LiPF_6$ in a solution of vinyl carbonate (EC) and diethyl carbonate (DEC) in a volume ratio of 1:1 was used as the electrolyte. The electrochemical properties were characterized by galvanostatic charge–discharge (GCD), cyclic voltammetry (CV), and electrochemical impedance spectroscopy (EIS). The CV data and the EIS data of the electrode capacity were recorded on a CHI600E system. The electrode capacity was measured on a Land CT2001A system. The scan rate of CV test is 0.1 $mV{\cdot}s^{-1}$ and potential range is 2.2–4.2 V. The range of EIS test frequency is 100 kHz–0.01 Hz and the voltage amplitude is 5 mV.

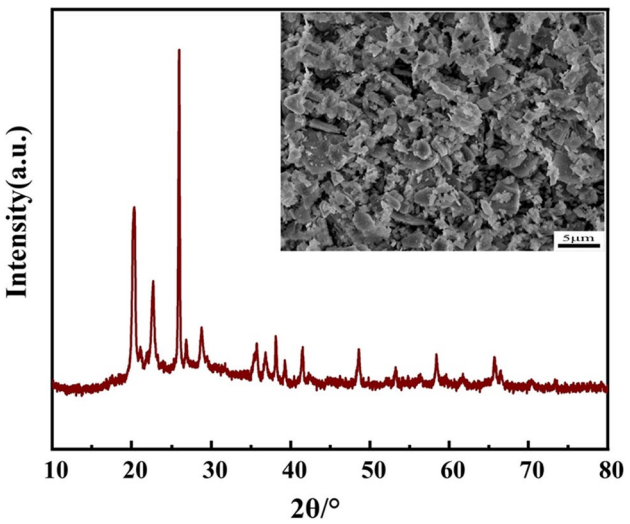

Fig. 1 Structural and morphological characterization of $FePO_4$

Results and discussion

The structural and morphological characterization of $FePO_4$ is shown in Fig. 1. It can be seen that $FePO_4$ has obvious characteristic diffraction peaks between diffraction angles of 20°–24°, which are basically consistent with the diffraction peaks of standard XRD. And the characteristic diffraction peak is high, which indicates that $FePO_4$ has high degree of crystallinity. The SEM image shows that the material has a fluffy layered structure, which can shorten the diffusion distance of Li^+ and ensure that Li^+ can enter into the lattice system of $FePO_4$ quickly. At the same time, the structure can increase the specific surface area and thus improve the electrochemical properties of the material.

The X-ray diffraction patterns of all the samples are given in Fig. 2. It is evident from the XRD curves that according to the standard pattern of JCPDF 83–2092, the five samples exhibit an olivine structure with no additional reflection peaks of impurities observed. Furthermore, the peaks associated with carbon are not observed in the XRD curves. It fully demonstrates that the obtained samples have a high

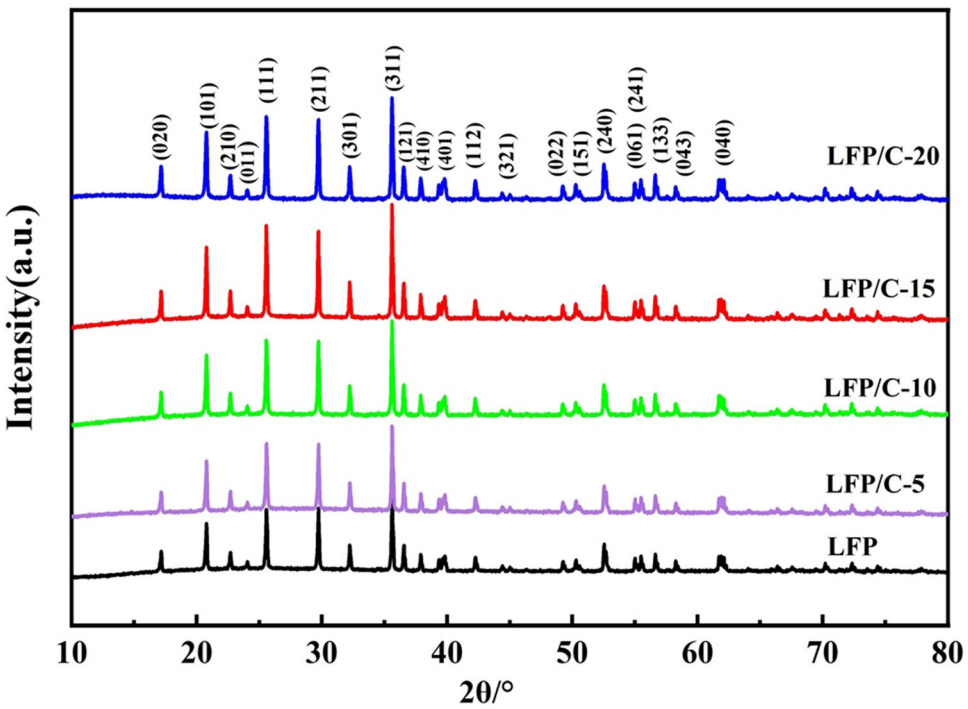

Fig. 2 XRD patterns of LFP/C composites of different carbon contents

purity and crystallinity. FWHM is usually used to reflect the size of particle size. According to the Scheller formula, the FWHM is inversely related to particle size. The FWHMs of the material at the positions of the sharpest diffraction peaks are 0.16098, 0.16384, 0.16591, 0.16803, and 0.16549, respectively, which fully demonstrates that the particle size of LFP/C-15 is the smallest. Meanwhile, it is clearly indicated in Fig. 2 that the diffraction peaks become more and more sharp as the carbon content increases and the peak height of the diffraction peaks is maximum when the carbon content is 15%, indicating the maximum crystallization of the material.

Figure 3 shows the SEM morphologies of the as-prepared materials. As shown in Fig. 3, glucose is uniformly dispersed on the surface of $LiFePO_4$ particles, showing a sphere-like morphology. Compared with LFP, LFP/C-5, and LFP/C-10, LFP/C-15 shows a significant reduction in particle size and a more uniform particle distribution; it is attributed to the fact that during the synthesis of LFP/C by carbothermal reduction, glucose is decomposed into carbon and thus wrapped around the surface of the LFP particles, which well prevents the agglomeration of particles. As the carbon content increases, a thin, homogeneous, and highly graphitized carbon film gradually forms, which restricts the increase in particle size. Meanwhile, the smaller the size of the sample, the greater the surface activity, resulting in greater repulsion between the particles, and thus a more uniform distribution of particles. However, Fig. 3(e) shows that with the carbon content increases excessively, LFP/C-20 has obvious particle agglomeration, because the content of active material is relatively low with high carbon content, which affects the vibrancy density of the material.

When the rate is set at 0.1 mV s^{-1}, the CV profiles of the five materials are shown in Fig. 4. Each of these curves is relatively similar, with an oxidation peak and a reduction peak, which correspond to the process of oxidation and reduction reactions of Fe^{2+}/Fe^{3+}. The potential separations of the prepared materials are 0.406 V, 0.395 V, 0.325 V, 0.322 V, and 0.400 V, respectively. Compared with other

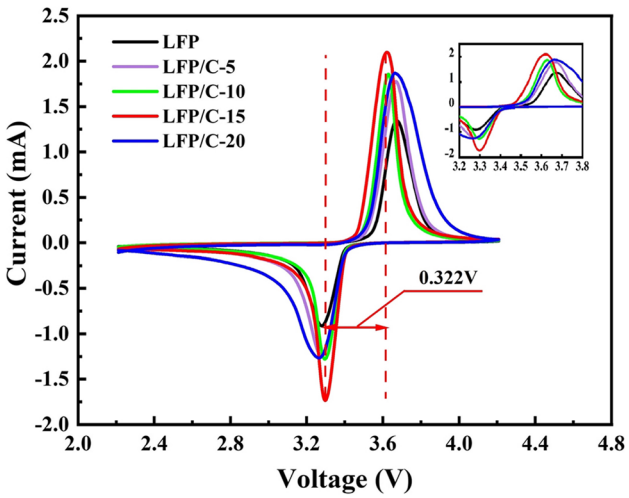

Fig. 4 CV curves of LFP/C composites of different carbon contents

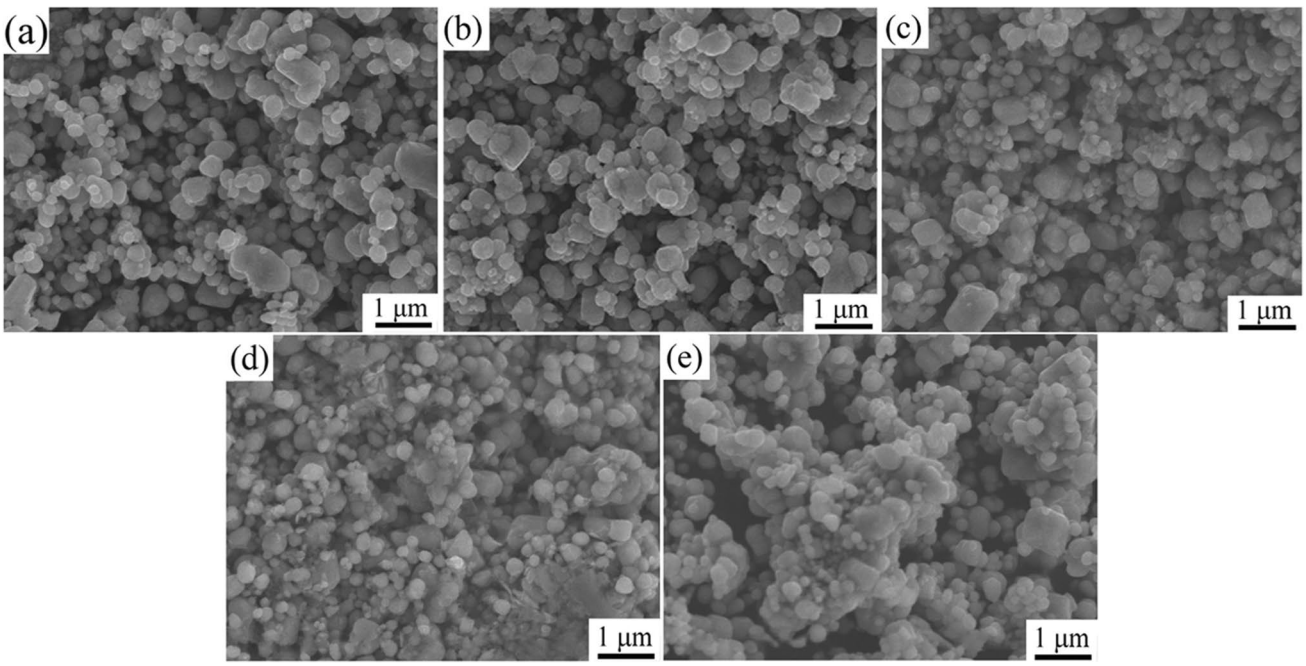

Fig. 3 SEM images of (**a**) LFP, (**b**) LFP/C-5, (**c**) LFP/C-10, (**d**) LFP/C-15, and (**e**) LFP/C-20

samples, LFP/C-15 shows a minimum potential separation of 0.322 V between the oxidation and reduction peaks, indicating a lower polarization during the electrochemical reaction. Meanwhile, LFP/C-15 exhibits the largest peak current and the maximum integral area consisting of the CV curves, which indicates that the electrode material by carbon coating has better electrochemical capacity and the carbon content is the most appropriate.

A systematic study of the effect of carbon content on the material properties is also investigated. Figure 5(a) exhibits the initial charge/discharge curves for all samples at 0.1 C. As noted, the initial discharge specific capacities of the prepared materials are 121.5, 137.6, 147.8, 160.7, and 137.7 mAh g^{-1}, respectively, and the coulombic efficiency of 101.0%, 99.5%, 100.1%, 99.5%, and 96.2%, respectively. It is obvious that LFP/C-15 shows the best performance and its initial discharge specific capacity is close to the theoretical specific capacity of LFP.

The cycle performance of all samples for 100 cycles at 0.1 C rate is presented in Fig. 5(b) and Table 1. Compared with the primitive LFP, the initial discharge capacity of LFP/C composite materials gradually rise with the increase of carbon content, due to forming a protective cover on the surface of LFP to prevent the chemical interaction with electrolyte. LFP/C-15 showed the highest discharge capacity of 131.5 mAh g^{-1}. When the carbon content is less than 15%, the charge and discharge performance decreases, which is attributed to the carbon content is too low and the effect of carbon coating is insufficient; the conductivity of LFP/C composite electrode material cannot be effectively improved. However, with the increase of carbon content, the cycle retention of the electrode materials decreases, due to the accumulation of carbon, which affects the capacity retention of the electrode materials.

Table 1 Cycling performance of LFP/C samples with different carbon contents

Samples	Initial discharge specific capacity (mAh g^{-1})	Final discharge specific capacity (mAh g^{-1})	Cycle retention (%)
LFP	122.9	105.8	86.1
LFP/C-5	137.8	115.1	83.5
LFP/C-10	151.8	125.6	82.7
LFP/C-15	160.1	131.5	82.1
LFP/C-20	142.7	116.1	81.4

Figure 5(c) and Table 2 present the rate performances of all samples at different rates from 0.1 to 2 C. It can be observed that the trend is opposite when the discharge capacity varies with the current density and the trend of downward is particularly significant under high current rate. The discharge capacity increases with the increase of carbon content, but the discharge capacity decreases significantly when the carbon content exceeds 15%. The composite material with 15% carbon content displays the highest capacity. It can achieve a capacity of 164.5, 160.7, 152.1, 141.7, and 124.9 mAh g^{-1} at 0.1 C, 0.2 C, 0.5 C, 1 C, and 2 C, respectively.

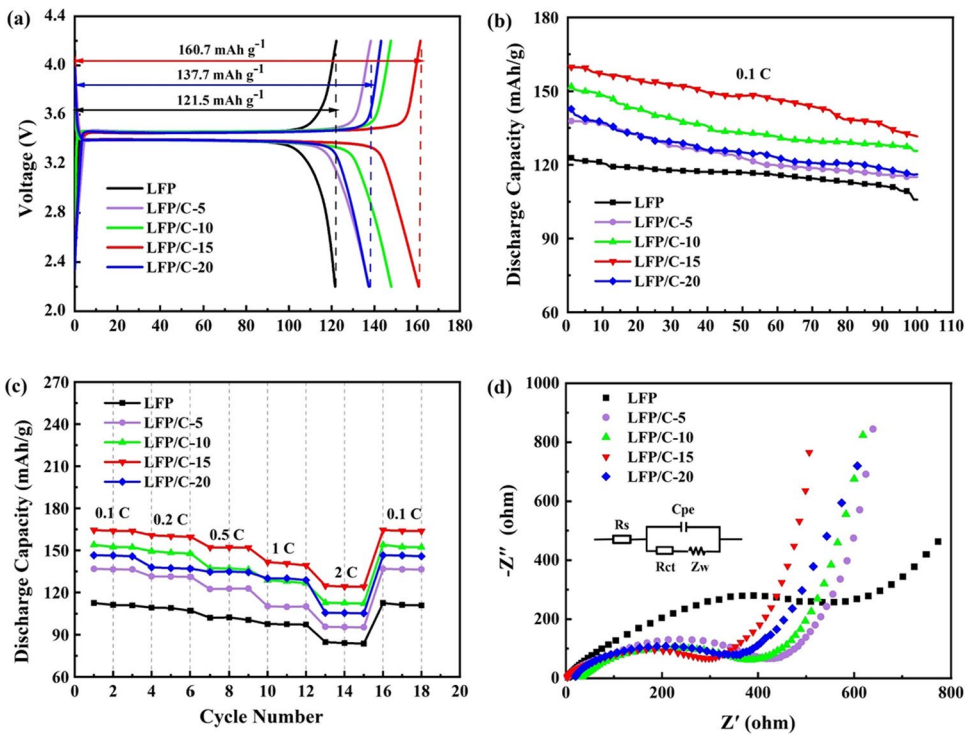

Fig. 5 Electrochemical performance of LFP/C composites of different carbon contents. (**a**) The first charging and discharging profiles of LFP/C at 0.1 C. (**b**) Cycle performance of LFP/C at 0.1 C. (**c**) Rate performance of LFP/C at 0.1 C. (**d**) Nyquist plots

Table 2 Rate performance of LFP/C samples with different carbon contents

Samples	Specific capacity at different discharge rates (mAh g^{-1})				
	0.1 C	0.2 C	0.5 C	1 C	2 C
LFP	112.5	109.2	102.1	97.5	84.7
LFP/C-5	136.8	131.4	122.4	110.2	95.6
LFP/C-10	154.0	149.4	137.2	128.8	112.7
LFP/C-15	164.5	160.7	152.1	141.7	124.9
LFP/C-20	146.5	137.9	134.7	130.0	105.6

To further investigate the electrochemical properties of the samples, the electrochemical impedance spectroscopy (EIS) of the samples are shown in Fig. 5(d). It is visualized from the Nyquist curves that each curve is composed of a depressed semicircle and a straight line, representing the process of charge transfer and Warburg diffusion, respectively. According to the fitting results, the values of the charge transfer resistance (R_{ct}) of all samples are 557 Ω, 432 Ω, 392 Ω, 304 Ω, and 355 Ω, respectively. Due to the improved electrical conductivity by carbon coating, compared with primitive LFP, the semicircular arc radius of other samples is smaller and the slope of other samples is higher. It is obvious that the semicircular arc radius of the LFP/C-15 is the smallest and the slope is the highest. Therefore, it shows that the internal resistance of LFP/C-15 is the smallest and the ion exchange behavior during charge and discharge is the fastest. However, the R_{ct} of LFP/C-20 increases in contrast due to the agglomeration of particles.

Conclusion

In this work, we successfully prepared LFP/C composites with different carbon contents by carbothermal reduction method, and demonstrated that proper carbon content can significantly enhance the material properties. As the carbon content increases, the effect on the material varies. The morphological characterization shows that the particle size of LFP/C-15 is smaller and the particle distribution is more uniform. Meanwhile, electrochemical characterization indicates that LFP/C-15 exhibits the highest specific discharge capacity as well as the best cycling stability among all samples. The discharge capacity of LFP/C-15 was 160.7 mAh g^{-1} after 100 cycles at 0.1 C, with a capacity retention rate of 82.1%. The performance of the material decreases in contrast when the carbon content exceeds 15%. The above results show that the proper amount of carbon forms a good conductive layer, which limits the size of the particles and greatly improves the electrical conductivity. It also proves that the carbon content is a very critical factor in improving the material properties.

Declarations

Conflict of interest The authors declare no competing interests.

References

1. Yang X, Tu J, Lei M, Zuo Z, Wu B, Zhou H (2016) Selection of carbon sources for enhancing 3D conductivity in the secondary structure of $LiFePO_4$/C cathode. Electrochimica Acta 193:206–215. https://doi.org/10.1016/j.electacta.2016.02.068
2. Gao C, Zhou J, Liu G, Wang L (2017) Synthesis of F-doped $LiFePO_4$/C cathode materials for high performance lithium-ion batteries using co-precipitation method with hydrofluoric acid source. J Alloys Compd 727:501–513. https://doi.org/10.1016/j.jallcom.2017.08.149
3. Hong S-A, Kim DH, Chung KY, Chang W, Yoo J, Kim J (2014) Toward uniform and ultrathin carbon layer coating on lithium iron phosphate using liquid carbon dioxide for enhanced electrochemical performance. J Power Sources 262:219–223. https://doi.org/10.1016/j.jpowsour.2014.03.132
4. Lim J, Gim J, Song J, Nguyen DT, Kim S, Jo J, Mathew V, Kim J (2016) Direct formation of $LiFePO_4$/graphene composite via microwave-assisted polyol process. J Power Sources 304:354–359. https://doi.org/10.1016/j.jpowsour.2015.11.069
5. Schmuch R, Wagner R, Hörpel G, Placke T, Winter M (2018) Performance and cost of materials for lithium-based rechargeable automotive batteries. Nat Energy 3:267–278. https://doi.org/10.1038/s41560-018-0107-2
6. Tian Z, Liu S, Ye F, Yao S, Zhou Z, Wang S (2014) Synthesis and characterization of $LiFePO_4$ electrode materials coated by graphene. App Surf Sci 305:427–432. https://doi.org/10.1016/j.apsusc.2014.03.106
7. Wang Q, Peng D, Chen Y, Xia X, Liu H, He Y, Ma Q (2018) A facile surfactant-assisted self-assembly of $LiFePO_4$/graphene composites with improved rate performance for lithium ion batteries. J of Electroanal Chem 818:68–75. https://doi.org/10.1016/j.jelechem.2018.04.030
8. Adepoju AA, Williams QL (2020) High C-rate performance of $LiFePO_4$/carbon nanofibers composite cathode for Li-ion batteries. Curr App Phys 20:1–4. https://doi.org/10.1016/j.cap.2019.09.014
9. Du G, Zhou Y, Tian X, Wu G, Xi Y, Zhao S (2018) High-performance 3D directional porous $LiFePO_4$/C materials synthesized by freeze casting. App Surf Sci 453:493–501. https://doi.org/10.1016/j.apsusc.2018.05.142
10. Huang C, Ai D, Wang L, He X (2013) Rapid synthesis of $LiFePO_4$ by coprecipitation. Chem Lett 42:1191–1193. https://doi.org/10.1246/cl.130436
11. Wei X, Guan Y, Zheng X, Zhu Q, Shen J, Qiao N, Zhou S, Xu B (2018) Improvement on high rate performance of $LiFePO_4$ cathodes using graphene as a conductive agent. Appl Surf Sci 440:748–754. https://doi.org/10.1016/j.apsusc.2018.01.201
12. Li D, Huang Y, Sharma N, Chen Z, Jia D, Guo Z (2012) Enhanced electrochemical properties of $LiFePO_4$ by Mo-substitution and graphitic carbon-coating via a facile and fast microwave-assisted solid-state reaction. Phys Chem Chem Phys 14:3634–3639. https://doi.org/10.1039/c2cp24062a
13. Shi M, Kong L-B, Liu J-B, Yan K, Li J-J, Dai Y-H, Luo Y-C, Kang L (2015) A novel carbon source coated on C-$LiFePO_4$ as a cathode material for lithium-ion batteries. Ionics 22:185–192. https://doi.org/10.1007/s11581-015-1549-1
14. Wang X, Huang Y, Jia D, Guo Z, Ni D, Miao M (2010) Preparation and characterization of high-rate and long-cycle $LiFePO_4$/C

nanocomposite as cathode material for lithium-ion battery. J Solid State Electrochem 16:17–24. https://doi.org/10.1007/s10008-010-1269-4
15. Yi X, Zhang F, Zhang B, Yu W-J, Dai Q, Hu S, He W, Tong H, Zheng J, Liao J (2018) (010) facets dominated $LiFePO_4$ nanoflakes confined in 3D porous graphene network as a high-performance Li-ion battery cathode. Ceram In 44:18181–18188. https://doi.org/10.1016/j.ceramint.2018.07.026
16. Gong H, Xue H, Wang T, He J (2016) In-situ synthesis of monodisperse micro-nanospherical $LiFePO_4$ /carbon cathode composites for lithium-ion batteries. J Power Sour 318:220–227. https://doi.org/10.1016/j.jpowsour.2016.03.100
17. Su C, Bu X, Xu L, Liu J, Zhang C (2012) A novel $LiFePO_4$/graphene/carbon composite as a performance-improved cathode material for lithium-ion batteries. Electrochimica Acta 64:190–195. https://doi.org/10.1016/j.electacta.2012.01.014
18. Tian X, Zhou Y, Wu G, Wang P, Chen J (2017) Controllable synthesis of porous $LiFePO_4$ for tunable electrochemical Li-insertion performance. Electrochimica Acta 229:316–324. https://doi.org/10.1016/j.electacta.2017.01.093
19. Wu K, Hu G, Du K, Peng Z, Cao Y (2015) Improved electrochemical properties of $LiFePO_4$/graphene/carbon composite synthesized from $FePO_4{\cdot}2H_2O$/graphene oxide. Ceram Int 41:13867–13871. https://doi.org/10.1016/j.ceramint.2015.06.130
20. Yang C-C, Hsu Y-H, Shih J-Y, Wu Y-S, Karuppiah C, Liou T-H, Lue SJ (2017) Preparation of 3D micro/mesoporous $LiFePO_4$ composite wrapping with porous graphene oxide for high-power lithium ion battery. Electrochimica Acta 258:773–785. https://doi.org/10.1016/j.electacta.2017.11.126
21. Liu T, Cao F, Ren L, Li X, Sun S, Sun X, Zang Z, Niu Q, Wu J (2017) A theoretical study of different carbon coatings effect on the depolarization effect and electrochemical performance of $LiFePO_4$ cathode. J Electroanal Chem 807:52–58. https://doi.org/10.1016/j.jelechem.2017.11.021
22. Zhang K, Lee JT, Li P, Kang B, Kim JH, Yi GR, Park JH (2015) Conformal coating strategy comprising N-doped carbon and conventional graphene for achieving ultrahigh power and cyclability of $LiFePO_4$. Nano Lett 15:6756–6763. https://doi.org/10.1021/acs.nanolett.5b02604
23. Ni J, Zhao Y, Chen J, Gao L, Lu L (2014) Site-dependent electrochemical performance of Mg doped $LiFePO_4$. Electrochem Commun 44:4–7. https://doi.org/10.1016/j.elecom.2014.04.004
24. Liu Y, Gu Y-J, Luo G-Y, Chen Z-L, Wu F-Z, Dai X-Y, Mai Y, Li J-Q (2020) Ni-doped $LiFePO_4$/C as high-performance cathode composites for Li-ion batteries. Ceram Int 46:14857–14863. https://doi.org/10.1016/j.ceramint.2020.03.011
25. Khan S, Raj RP, Mohan TVR, Bhuvaneswari S, Varadaraju UV, Selvam P (2019) Electrochemical performance of nano-$LiFePO_4$ embedded ordered mesoporous nitrogenous carbon composite as cathode material for Li-ion battery applications. J Electroanal Chem 848:113242–113251. https://doi.org/10.1016/j.jelechem.2019.113242